Twenty-One Millisecond Pulsars in Terzan 5 Using the Green Bank Telescope

Scott M. Ransom,[1,2]* Jason W. T. Hessels,[2] Ingrid H. Stairs,[3] Paulo C. C. Freire,[4] Fernando Camilo,[5] Victoria M. Kaspi,[2] David L. Kaplan[6]

We have identified 21 millisecond pulsars (MSPs) in globular cluster Terzan 5 by using the Green Bank Telescope, bringing the total of known MSPs in Terzan 5 to 24. These discoveries confirm fundamental predictions of globular cluster and binary system evolution. Thirteen of the new MSPs are in binaries, of which two show eclipses and two have highly eccentric orbits. The relativistic periastron advance for the two eccentric systems indicates that at least one of these pulsars has a mass 1.68 times greater than the mass of the Sun at 95% confidence. Such large neutron star masses constrain the equation of state of matter at or beyond the nuclear equilibrium density.

The extremely high stellar densities (10^4 to 10^6 pc^{-3}) in the cores of globular clusters (GCs) result in stellar interactions that produce and destroy binary systems as well as exchange their members (*1*). Formed by the death of massive stars early in a cluster's history, neutron stars (NSs) usually reside near the cores of clusters because of their relatively large masses and the mass segregation induced by dynamical friction. There they are likely to interact with one or more stars over the 10^{10}-year lifetimes of GCs. These interactions lead to a production rate of low-mass x-ray binaries (LMXBs) and their progeny such as MSPs [via the recycling mechanism (*2*)] that is highly enhanced compared with the rate in the Milky Way Galaxy. Before our observations, there were 80 pulsars (most of them binary MSPs) known in 24 GCs (*3*), with the relatively massive and nearby cluster 47 Tucanae containing 22 of these (*4*). Finding and monitoring many pulsars in a single cluster provides unique probes into a range of GC, binary evolutionary, and stellar astrophysics (*5*, *6*). In addition, GCs produce exotic systems such as highly eccentric (*7*) and MSP−main sequence star binaries (*8*).

The interaction rate between NSs and other stars or binaries in a GC is a complex function of the total cluster mass, the size of the cluster core (*9*) and its stellar density, the initial stellar mass function, and the level of mass segregation present in the cluster (*10*). However, relatively simple theoretical modeling of stellar interaction rates (*11*), as well as one known LMXB and several additional x-ray sources detected recently with the Chandra X-ray Observatory (*12*), indicate that the dense, massive, and metal-rich GC Terzan 5 has one of the highest stellar interaction rates of any cluster in the Galaxy (*13*) and perhaps also the largest number of MSPs (*14*, *15*). But because Terzan 5 [Galactic coordinates (l, b) = (3.8°, 1.7°)] is distant (D = 8.7 ± 2 kpc) and located within ~1 kpc of the Galactic center (*16*), the large column density of interstellar free electrons (i.e., the dispersion measure, DM ~ 240 pc cm^{-3}) produces considerable dispersive smearing ($\propto \nu^{-3}$ for typical pulsar search data) and scatter broadening ($\propto \nu^{-4.4}$) of radio pulses, which hinders pulsation searches for MSPs at the often-observed radio frequencies (ν) of 400 to 1400 MHz.

Deep radio images of Terzan 5, which are not affected by the dispersive effects of the interstellar medium (ISM), were made with the Very Large Array (VLA) and showed what appeared to be the integrated emission from many tens or even hundreds of pulsars with low flux densities (*17*). Surprisingly, numerous deep searches for pulsars over the past 15 years using the Parkes radio telescope at 1400 MHz have identified only three (*18*): the 11-ms Ter 5 A with its unusual eclipses (*19*) and the two isolated MSPs Ter 5 C (*20*) and D (*21*).

Observations and data analysis. On 17 July 2004, we observed Terzan 5 for 5.9 hours with the National Radio Astronomy Observatory's (*22*) 100-m Green Bank Telescope (GBT) and the Pulsar Spigot backend (*23*). The S-band receiver provided 600 MHz (1650 to 2250 MHz) of relatively interference-free bandwidth in two orthogonal polarizations, which the Spigot summed and synthesized into 768 0.78125-MHz frequency channels every 81.92 μs. With the known DM and scattering time scale (*24*) toward the cluster, the effective time resolution of the data was ~0.3 ms. We observed only a single position, because the 6.5′ telescope beam width at these frequencies is much larger than the 0.83′ half-mass radius of the cluster (*25*). The large unblocked aperture of the GBT, the wide bandwidth provided by the Spigot and the S-band receiver, and the move to higher observing frequencies together provided an increase in sensitivity over the Parkes searches (*21*) by factors of ~5 for typical recycled pulsars and by ≳10 for MSPs with spin periods $P_{psr} \lesssim 2$ ms (*26*).

We searched the observation by dedispersing the raw data into 40 separate time series with DMs ranging from 230 to 250 pc cm^{-3} and spaced by 0.5 pc cm^{-3}. We Fourier-transformed the full 5.9-hour time series as well as 10-, 20-, and 60-min sections and searched them by using Fourier-domain acceleration search techniques (*27*) in a manner similar to that described in (*28*) in order to maintain sensitivity to pulsars in compact binary systems. In that first observation, we detected 14 new pulsars, Ter 5 E to R (*29*). By using eight more observations taken between July and November 2004, we found seven additional pulsars and determined the basic orbital parameters of 10 of the 13 new binaries (Fig. 1 and Table 1). In general, the uncalibrated flux densities of the pulsars (as computed by comparing the integrated signal from a pulsar to the predicted total system noise level) were constant to within a level of ≲50% between these observations, implying that diffractive scintillation will not largely affect pulsar measurements for Terzan 5 at these observing frequencies. Several additional binary pulsar candidates from these data remain unconfirmed but may reappear in future observations at more fortuitous orbital phases. Because the volume enclosed by the GBT beam at 1950 MHz out to a distance of 10 kpc is ~10^{-3} kpc^3 and it has been estimated (*30*) that there are roughly 10^5 observable MSPs within the Galaxy (with volume ~ 10^2 to 10^3 kpc^3), it is possible that a detectable foreground MSP is within our beam. However, given that the DM toward Terzan 5 is known

[1]National Radio Astronomy Observatory, 520 Edgemont Road, Charlottesville, VA 22903, USA. [2]Department of Physics, McGill University, 3600 University Street, Montreal, QC H3A 2T8, Canada. [3]Department of Physics and Astronomy, University of British Columbia, 6224 Agricultural Road, Vancouver, BC V6T 1Z1, Canada. [4]National Astronomy and Ionosphere Center, Arecibo Observatory, HC03 Box 53995, PR 00612, USA. [5]Columbia Astrophysics Laboratory, Columbia University, 550 West 120th Street, New York, NY 10027, USA. [6]Center for Space Research, Massachusetts Institute of Technology, 70 Vassar Street, Cambridge, MA 02139, USA.

*To whom correspondence should be addressed. E-mail: sransom@nrao.edu

to within ~5%, the probability of that MSP having a similar DM is much smaller, and hence we are confident that all of the new pulsars are members of Terzan 5. Positions with arc sec accuracy of the new MSPs from pulsar timing will solidify the associations.

The new pulsar population. With our initial discovery data, the ensemble of pulsars all have measured DMs with errors $\lesssim$ 0.1 pc cm^{-3}, flux densities, S_{1950}, with fractional errors of ~30%, and precisely determined P_{psr} values. These measurements allow us to compare the new systems with known MSPs such as those in 47 Tuc. Once precise positions and pulsar spin period derivatives have been determined from timing observations over the next year (the positions of the new pulsars are currently known only to within the 6.5′ primary beam of the GBT), a variety of tests of the gravitational potential and internal dynamics of Terzan 5 will be possible, in addition to estimates of the ages and magnetic field strengths of many of the pulsars (*31*).

The DMs for the pulsars in Terzan 5 are distributed with a central Gaussian-like component having an average and standard deviation of 237.8 ± 1.4 pc cm^{-3} and five outliers having higher and lower DMs (Table 1). The overall spread in DM, 9.5 pc cm^{-3} (13 times larger than what is observed for 47 Tuc), is the largest known for any GC and is likely due to the large average DM for Terzan 5 and irregularities in the ISM along the differing sight lines toward its pulsars. The Gaussian-like component of the DM distribution likely corresponds to a group of centrally concentrated pulsars near the cluster core. The position of Ter 5 C, which has an average DM, is about 10″ or one core radius (*9*) north of the cluster center and supports such a notion. Likewise, pulsars with outlying DMs, such as Ter 5 D and J, are probably more offset like Ter 5 A, which has a high DM and is located 36″ from the center (*20*).

The VLA radio imaging of Terzan 5 (*17*) revealed numerous point sources within 30″ of the cluster center, as well as ~2 mJy (1 Jy = 10^{-26} W m^{-2} Hz^{-1}) of diffuse emission at 1400 MHz within ~10″. The central emission was attributed to 60 to 200 unresolved pulsars assuming D = 7.1 kpc, a standard luminosity distribution, and a minimum pulsar luminosity ($L_{1400} \equiv S_{1400}D^2$) of $L_{1400,min}$ = 0.3 mJy kpc^2. A distance to Terzan 5 of D = 8.7 kpc (*16*) would increase the number of unresolved pulsars by ~50%. For a typical pulsar radio spectral index of −1.6 (*32*) and omitting the flux densities of Ter 5 A and C, which are located outside the region of diffuse emission (*20*), the integrated measured flux density from the other 22 pulsars at 1400 MHz is ~1.3 mJy. If the five pulsars with outlying DMs reside outside the cluster core, the total flux density from the remaining pulsars is only ~1 mJy. None of the new pulsars can individually (or in combination with nearby Ter 5 C) account for the bright (1.42 mJy) point source ''N'' located 12″ north of the cluster center (*17*). However, given its very wide pulse profile, lack of a flat off-pulse baseline, and positional coincidence (*20*), Ter 5 C could possibly emit substantial unpulsed emission like MSP J0218+4232 (*33*) and thereby account for all of the flux density of source N.

The differential luminosity distribution of the new pulsars resembles that of the 47 Tuc (*4*), M15 (*5*), and the Galactic disk (*34*) populations by following the normal $d\log N =$

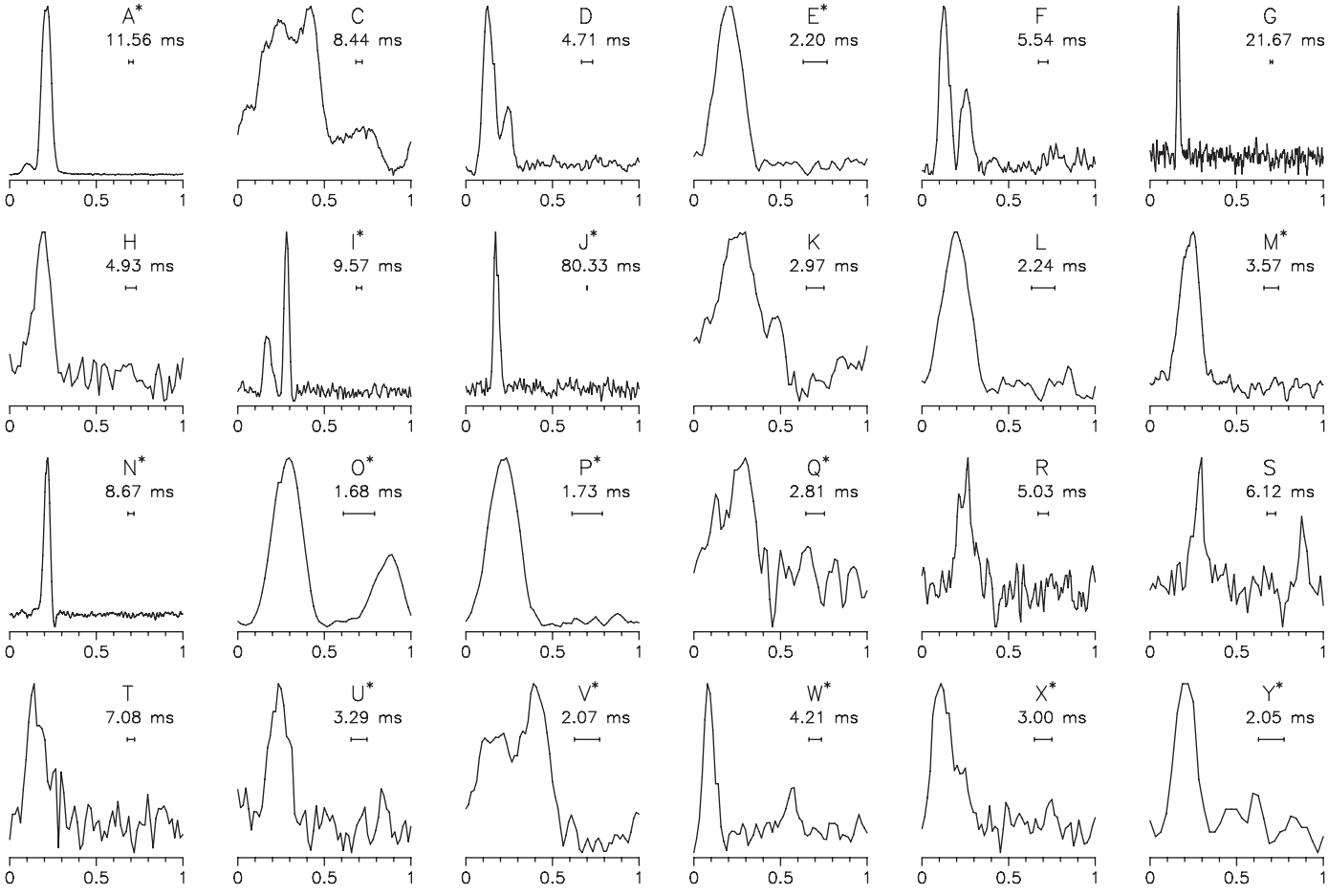

Fig. 1. The 1950 MHz GBT+Spigot pulse profiles for each of the pulsars known in Terzan 5. All but Ter 5 A, C, and D are newly discovered (*18*). Each profile is the weighted average of the best detections of that pulsar and is a measure of the relative flux density as a function of rotational phase. Asterisks indicate that the pulsar is the member of a binary system, and the length of the horizontal error bar (0.3 ms) is the effective system time resolution.

$-d\log L$ relation, with no sign of a downturn at the low luminosity end ($L_{1400} \sim 1$ to 2 mJy kpc^2). This implies that we have not reached the lowest luminosities of the intrinsic pulsar distribution in Terzan 5, nor have we yet reached the sensitivity limit of the observing system (*35*). It is likely that tens of less-luminous pulsars remain to be discovered in Terzan 5, possibly even several bright ones (e.g., the source N). Such bright pulsars may remain undetected if they are members of very compact or massive binaries due to eclipsing or excessive doppler accelerations or if they have extremely fast spin periods ($P_{psr} \ll 1.5$ ms). Detailed searches using more advanced search techniques may yet uncover these systems.

The 24 known pulsars in Terzan 5 and the 22 in 47 Tuc appear to have different spin period distributions. The 47 Tuc pulsars are a homogeneous population with periods from 2.1 to 7.6 ms (*3*), whereas those in Terzan 5 have a flatter distribution that includes six pulsars slower than 7.6 ms and the four fastest pulsars known in GCs (P_{psr} values of 1.67, 1.73, 2.05, and 2.07 ms). A Kolmogorov-Smirnov test suggests that these samples are drawn from different parent distributions at 85% confidence. These differences may be related to the dynamical states of the cluster cores [i.e., just pre- or just postcore collapse for Terzan 5 (*16*)], different epochs of MSP creation, or the occurrence of unusual evolutionary mechanisms that only manifest themselves at very high (i.e., $>10^5$ pc^{-3}) stellar densities.

Individual pulsars. The binaries Ter 5 E and W have orbital periods, P_{orb}, of ~60 days and ~4.9 days, respectively. In the dense stellar environment of a GC, such wide binaries have large cross sections for stellar encounters that can disrupt them, eject them from the cluster core, or, after multiple collisions, induce eccentricity (*36*) in their initially circular orbits (*31*). For these pulsars, the measured eccentricities are $e \sim 0.02$, substantially larger than those predicted for binary MSPs with helium white dwarf (WD) companions in the Galaxy (*31*). If they are located near the cluster center, where the stellar densities are $\gtrsim 10^5$ pc^{-3} (*25*), the time scale for interactions to produce such eccentricities is 10^8 to 10^9 years (*36*), consistent with the $\gtrsim 10^9$-year ages of most cluster pulsars. However, the 60-day orbit of Ter 5 E implies a time scale near the low end of that range, possibly too short for MSP lifetimes. This may indicate that it resides further from the center of Terzan 5: More than 10^9 years spent in the core could result in many interactions that would either destroy the binary or induce much larger eccentricities. The eccentricities of Ter 5 I and J are too large to have been produced by this method, especially given the relatively compact nature of their orbits, indicating that they were formed by a different mechanism.

Table 1. Known pulsars in Terzan 5 (*18*). Pulsars listed without orbital parameters are likely isolated systems, whereas those marked with an *e* are eclipsing systems. The errors on the dispersion measures (DMs) range from 0.01 to 0.1 pc cm^{-3}, and the errors on the measured flux densities are ~30%. The flux densities for the eclipsing pulsars include only the times when the pulsar is not eclipsed. The light travel time across the projected pulsar semimajor axis is defined as $x \equiv a_1 \sin(i)/c$. Eccentricities listed as "0" are too small to measure at present and have been set to zero for orbital parameter fitting. The minimum companion mass m_2 was calculated assuming a pulsar mass m_1 of 1.4 $M_\odot$ and $i = 90°$ except for Ter 5 I and J (Fig. 2). All measured parameters were determined with the use of the Tempo software package (*47*). Unk., unknown.

PSR	P_{psr} (ms)	Dispersion measure (pc cm^{-3})	1950 MHz flux density (μJy)	P_{orb} (days)	x (lt-s)	Eccentricity	Minimum m_2 ($M_\odot$)
A[e]	11.56315	242.44	1020	0.0756	0.120	0	0.089
C	8.43610	237.14	360				
D	4.71398	243.83	41				
E	2.19780	236.84	48	60.06	23.6	~ 0.02	0.22
F	5.54014	239.18	35				
G	21.67187	237.57	15				
H	4.92589	238.13	15				
I	9.57019	238.73	29	1.328	1.818	0.428	0.24
J	80.33793	234.35	19	1.102	2.454	0.350	0.38
K	2.96965	234.81	40				
L	2.24470	237.74	41				
M	3.56957	238.65	33	0.4431	0.596	0	0.14
N	8.66690	238.47	55	0.3855	1.619	0.000045	0.48
O[e]	1.67663	236.38	120	0.2595	0.112	0	0.036
P[e]	1.72862	238.79	77	0.3626	1.272	0	0.38
Q	2.812	234.50	27	> 1?	Unk.	Unk.	Unk.
R	5.02854	237.60	12				
S	6.11664	236.26	18				
T	7.08491	237.70	20				
U	3.289	235.50	16	> 1?	Unk.	Unk.	Unk.
V	2.07251	239.11	71	0.5036	0.567	0	0.12
W	4.20518	239.14	22	4.877	5.869	0.015	0.30
X	2.999	240.03	18	> 1?	Unk.	Unk.	Unk.
Y	2.04816	239.11	16	1.17	1.16	0	0.14

At least two of the new binary pulsars, Ter 5 O and P, have been observed to eclipse, although given the factor of 10 difference in the inferred companion masses ($m_2 \gtrsim 0.036\ M_\odot$ for Ter 5 O and $\gtrsim 0.38\ M_\odot$ for Ter 5 P, where $M_\odot$ is the mass of the Sun) and eclipse durations ($\sim 0.05 P_{orb}$ for Ter 5 O and $\gtrsim 0.5 P_{orb}$ for Ter 5 P), the systems are unalike. Ter 5 O, the third fastest MSP known, is similar to the Black-Widow eclipsing MSP B1957+20 (*37*), with a very low-mass companion and an eclipse duration (~ 15 to 20 min) corresponding to a physical size (~0.03 $R_\odot$, where $R_\odot$ is the radius of the Sun) much larger than the companion star's Roche lobe. Such systems are common in GCs (*38*). Ter 5 P, the fourth fastest MSP known, is unusual and most similar to the binary MSP NGC 6397 A, whose peculiar red straggler or sub-subgiant companion causes irregular and long-duration eclipses of the radio pulses (*8*). Ter 5 P's eclipses are also irregular and correspond to an eclipsing region of several solar radii in size, indicating the companion is likely a peculiar evolved star as well. If so, the system may have been created after at least one exchange encounter where the MSP's original companion (which had spun up the pulsar) was ejected and replaced by a main sequence star. Such an encounter might eject the system from the core of the cluster, as has been observed for NGC 6397 A [although alternative formation scenarios for this pulsar have been proposed as well (*39*)].

The pulsars Ter 5 I and J are in highly eccentric orbits with companions of at least 0.24 and 0.38 $M_\odot$, respectively (Fig. 2). The companions are not sufficiently massive to be NSs unless the systems have improbably low inclination angles i (i.e., are almost face-on). If they were main-sequence or giant stars, eclipses would likely be observed for a variety of inclinations given the compactness of the orbits (orbital separations of ~5 $R_\odot$). Additionally, the orbital circularization time scales would be on the order of 10^5 years for both pulsars and so no eccentricity should currently be observed (*40*). The companions are therefore probably WDs. However, the pulsar recycling scenario generates MSP-WD binaries in nearly circular orbits because of tidal interactions during mass transfer and therefore did not produce these eccentric systems. A possible scenario involves the off-center collision of a NS with a red giant, which would disrupt the giant's envelope

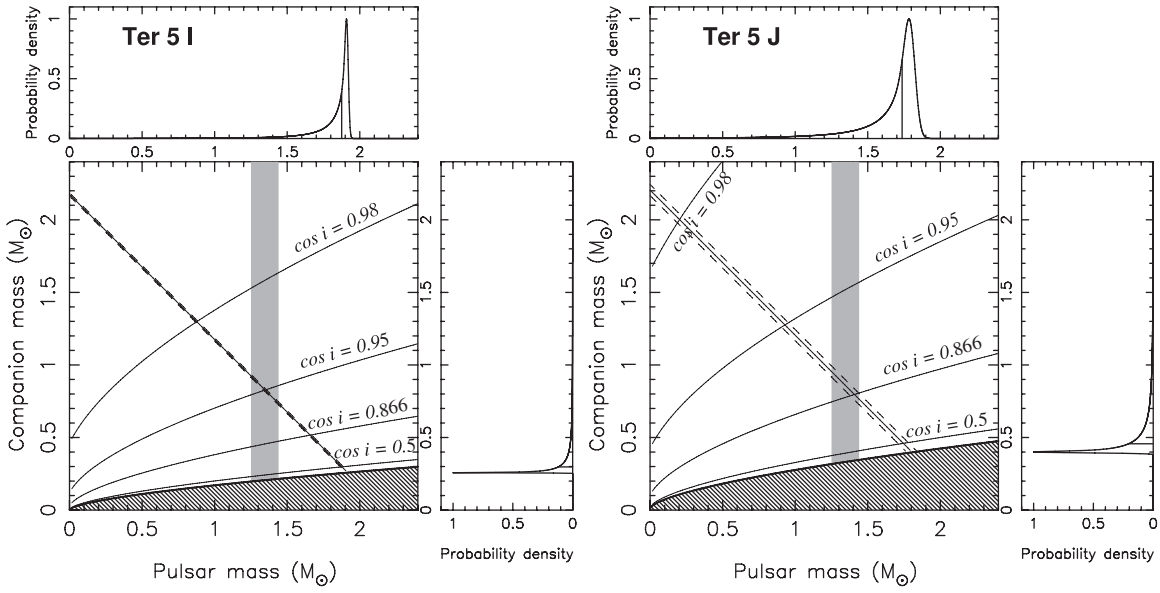

Fig. 2. Pulsar mass versus companion mass diagrams for the two highly eccentric binary pulsars Ter 5 I (**left**) and Ter 5 J (**right**). The hatched regions are excluded because of the definition of the Keplerian mass function (i.e., $\sin i \leq 1$). The diagonal band in the center of the figure shows the total system mass with 1σ confidence intervals as measured by the general-relativistic advance of periastron $\dot{\omega} = 0.255 \pm 0.001°$ year^{-1} for I and $\dot{\omega} = 0.327 \pm 0.004°$ year^{-1} for J. The marginal distributions show the masses of the pulsars and companions assuming a random distribution of inclinations (i.e., with probability density flat in cos *i*). The solid curves in the main plot indicate inclinations of (from top to bottom) 11.4°, 18.2°, 30°, 60°, and 90°. The gray vertical band shows the range of precisely measured NS masses from relativistic binary radio pulsars (*46*). In both cases, the median pulsar mass (indicated by the vertical line in the marginal distribution) lies significantly above 1.7 $M_\odot$, implying that one or both of these pulsars is considerably more massive than the NSs that have been well measured to date. A strict upper limit to the masses of both pulsars is 1.96 $M_\odot$.

and leave the core (now the WD) in an eccentric orbit about the NS (*41*). An alternative scenario involves the exchange of an initially isolated WD into a binary consisting of an MSP and the low-mass WD that recycled it. However, the observed pulsars are only mildly recycled. Furthermore, the multiple exchanges required in this scenario imply that the system was created near the core, where because of mass segregation the isolated WDs would be more massive than the observed companions to Ter 5 I and J. We therefore regard the collision scenario as more likely.

The high eccentricities of both orbits permitted us to measure their advances of the angle of periastron, $\dot{\omega} = 0.255 \pm 0.001°$ year^{-1} for I and $0.327 \pm 0.004°$ year^{-1} for J, which are likely caused by general-relativistic modification of the Keplerian elliptical orbit. Under this assumption, the total mass can be derived for each system: $2.17 \pm 0.02\ M_\odot$ for I and $2.20 \pm 0.04\ M_\odot$ for J. Together with the measured Keplerian mass functions in both cases, this result implies that the most likely NS masses are $> 1.7\ M_\odot$ (Fig. 2). However, classical contributions to $\dot{\omega}$ from tidal or rotational quadrupole mass moments in the companion star must also be considered (*42*, *43*). Tidal deformation is insignificant for a WD companion (*42*), but rotationally induced quadrupoles are possible if the WD is rapidly rotating, because there is no reason to expect the spin axis of the companion to be aligned with the orbital angular momentum.

The predicted contributions to $\dot{\omega}$ for Ter 5 I and J due to a rotationally induced quadrupole are $\dot{\omega}_{\rm rot} \sim 0.01$ to $0.02°$ year^{-1} times angular and stellar structure factors (*42*–*44*). One of the stellar structure factors, α_6, can range up to 15 for WDs (*42*), making $\dot{\omega}_{\rm rot}$ a potentially considerable contribution to the measured $\dot{\omega}$. A substantial $\dot{\omega}_{\rm rot}$, however, will produce changes in *i* and hence in the projected semimajor axis $x \equiv a_1 \sin(i)/c$. The size of this effect may be written as $\dot{\omega}_{\rm rot} \sim \dot{x}_{\rm rot}/x$ times a trigonometric factor usually of order unity that depends on *i*, the angle between the WD rotation axis and the orbital angular momentum vector, and the phase of the orbital precession (*43*). For random choices of these angles, the trigonometric factor is <10 ~80% of the time. By incorporating detections from Parkes search observations taken in 1998 and 2000 (*21*) with the use of the now-known orbital ephemerides, we have upper limits on $\dot{x}$, which imply that $\dot{\omega}_{\rm rot}$ is $\lesssim 0.003°$ year^{-1} times the trigonometric factor for both systems. The magnitudes of these rotational-quadrupole contributions are comparable to our current measurement uncertainties for $\dot{\omega}$. We emphasize that this result does not depend on the type of companion and is equally valid for main-sequence stars and WDs. Therefore, unless the orientations of the orbital and rotational angular momentum vectors are fine-tuned for both systems, the $\dot{\omega}$ measurements are well described by general relativity. Under this assumption, one or both of these NSs are likely to be unprecedentedly massive: calculation of the joint probabilities (Fig. 2) indicates that at least one of the pulsars is more massive than 1.48, 1.68, or 1.74 $M_\odot$ at 99%, 95%, and 90% confidence levels, respectively. A strict upper limit to the masses of both pulsars is 1.96 $M_\odot$. Similar but slightly less stringent evidence from pulsar timing for a massive NS in the Galactic low-mass WD-MSP binary J0751+1807 has been presented (*45*). It is an intriguing question whether the large masses for Ter 5 I and J resulted from the collision formation mechanism, possibly during a short period of hypercritical accretion which partially or completely spun-up the pulsars (*41*). GBT observations over the next 1 to 3 years will measure the varying delays due to gravitational redshift and time dilation as Ter 5 I moves in its orbit, which together are known as γ (the measurement of γ for Ter 5 J will take 5 to 10 years because of the relatively slow spin period of the pulsar). This parameter, along with general relativity and the already well-measured $\dot{\omega}$, will provide a precise mass for the pulsar and will likely rule out several soft equations of state for matter at nuclear densities (*46*).

References and Notes

1. G. Meylan, D. C. Heggie, *Astron. Astrophys. Rev.* **8**, 1 (1997).
2. M. A. Alpar, A. F. Cheng, M. A. Ruderman, J. Shaham, *Nature* **300**, 728 (1982).
3. For an updated list, see www.naic.edu/~pfreire/GCpsr.html.
4. F. Camilo, D. R. Lorimer, P. Freire, A. G. Lyne, R. N. Manchester, *Astrophys. J.* **535**, 975 (2000).
5. S. B. Anderson, thesis, California Institute of Technology, Pasadena, CA (1992).
6. P. C. Freire *et al.*, *Mon. Not. R. Astron. Soc.* **340**, 1359 (2003).
7. P. C. Freire, Y. Gupta, S. M. Ransom, C. H. Ishwara-Chandra, *Astrophys. J.* **606**, L53 (2004).
8. N. D'Amico *et al.*, *Astrophys. J.* **561**, L89 (2001).
9. The core radius is defined as that where the optical surface brightness is half its central value.
10. F. Verbunt, in *New Horizons in Globular Cluster Astronomy*, F. Piotto, G. Meylan, S. G. Djorgovski, M. Riello, Eds. [Astronomical Society of the Pacific (ASP) Conference Series no. 296, ASP, San Francisco, CA, 2003], p. 245.

11. F. Verbunt, in *Omega Centauri, A Unique Window into Astrophysics*, F. van Leeuwen, J. D. Hughes, F. Piotto, Eds. (ASP Conference Series no. 265, ASP, San Francisco, CA, 2002), p. 289.
12. C. O. Heinke *et al.*, *Astrophys. J.* **590**, 809 (2003).
13. D. Pooley *et al.*, *Astrophys. J.* **591**, L131 (2003).
14. S. Sigurdsson, E. S. Phinney, *Astrophys. J. Suppl. Ser.* **99**, 609 (1995).
15. S. R. Kulkarni, S. B. Anderson, in *Dynamical Evolution of Star Clusters–Confrontation of Theory and Observations*, P. Hut, J. Makino, Eds. (International Astronomical Union Symposium no. 174, Kluwer, Dordrecht, Netherlands, 1996), p. 181.
16. H. N. Cohn, P. M. Lugger, J. E. Grindlay, P. D. Edmonds, *Astrophys. J.* **571**, 818 (2002).
17. A. S. Fruchter, W. M. Goss, *Astrophys. J.* **536**, 865 (2000).
18. The 442-ms pulsar J1748−2444 was initially identified as Ter 5 B (B1744−24B) but is now known to be a foreground pulsar unrelated to Terzan 5 (*20*).
19. A. G. Lyne *et al.*, *Nature* **347**, 650 (1990).
20. A. G. Lyne, S. H. Mankelow, J. F. Bell, R. N. Manchester, *Mon. Not. R. Astron. Soc.* **316**, 491 (2000).
21. S. M. Ransom, thesis, Harvard University, Cambridge, MA (2001).
22. The National Radio Astronomy Observatory is a facility of the National Science Foundation operated under cooperative agreement by Associated Universities, Incorporated.
23. D. Kaplan *et al.*, in preparation.
24. D. J. Nice, S. E. Thorsett, *Astrophys. J.* **397**, 249 (1992).
25. W. E. Harris, *Astron. J.* **112**, 1487 (1996).
26. These comparisons assume a typical pulsar spectral index of −1.6 (*32*).
27. S. M. Ransom, S. S. Eikenberry, J. Middleditch, *Astron. J.* **124**, 1788 (2002).
28. S. M. Ransom *et al.*, *Astrophys. J.* **604**, 328 (2004).
29. Ter 5 E was a candidate (i.e., unconfirmed) pulsar in (*21*).
30. A. G. Lyne *et al.*, *Mon. Not. R. Astron. Soc.* **295**, 743 (1998).
31. E. S. Phinney, S. R. Kulkarni, *Annu. Rev. Astron. Astrophys.* **32**, 591 (1994).
32. D. R. Lorimer, J. A. Yates, A. G. Lyne, D. M. Gould, *Mon. Not. R. Astron. Soc.* **273**, 411 (1995).
33. J. Navarro, G. de Bruyn, D. Frail, S. R. Kulkarni, A. G. Lyne, *Astrophys. J.* **455**, L55 (1995).
34. A. G. Lyne, R. N. Manchester, J. H. Taylor, *Mon. Not. R. Astron. Soc.* **213**, 613 (1985).
35. $S_{1950,\mathrm{min}}$ is about 8 μJy for $P \sim$ 2- to 4-ms isolated or long orbital period MSPs.
36. F. A. Rasio, D. C. Heggie, *Astrophys. J.* **445**, L133 (1995).
37. A. S. Fruchter, D. R. Stinebring, J. H. Taylor, *Nature* **333**, 237 (1988).
38. A. R. King, M. B. Davies, M. E. Beer, *Mon. Not. R. Astron. Soc.* **345**, 678 (2003).
39. A. Possenti *et al.*, in *Binary Radio Pulsars*, F. Rasio, I. Stairs, Eds. (ASP Conference Series no. 328, ASP, San Francisco, CA, 2005), p. 189.
40. J. Tassoul, *Astrophys. J.* **444**, 338 (1995).
41. F. A. Rasio, S. A. Shapiro, *Astrophys. J.* **377**, 559 (1991).
42. L. L. Smarr, R. Blandford, *Astrophys. J.* **207**, 574 (1976).
43. N. Wex, *Mon. Not. R. Astron. Soc.* **298**, 997 (1998).
44. E. M. Splaver *et al.*, *Astrophys. J.* **581**, 509 (2002).
45. D. J. Nice, E. M. Splaver, I. H. Stairs, in *Binary Radio Pulsars*, F. Rasio, I. Stairs, Eds. (ASP Conference Series no. 328, ASP, San Francisco, CA, 2005), p. 371.
46. J. M. Lattimer, M. Prakash, *Science* **304**, 536 (2004).
47. The Tempo program is available online at http://pulsar.princeton.edu/tempo.

48. We thank F. Rasio, S. Sigurdsson, and M. van Kerkwijk for extremely useful discussions and J. Herrnstein, L. Greenhill, D. Manchester, A. Lyne, and N. D'Amico for providing or aiding with the Parkes data from 1998 and 2000. J.W.T.H. is a Natural Sciences and Engineering Research Council of Canada (NSERC) Post-Graduate Scholarship–Doctoral fellow. I.H.S. holds an NSERC University Faculty Award and is supported by a Discovery grant and University of British Columbia start-up funds. F.C. thanks support from NSF. V.M.K. holds a Canada Research Chair and is supported by an NSERC Discovery Grant and Steacie Fellowship Supplement, by the Fonds Québécois de la recherche sur la nature et les technologies and Canadian Institute for Advanced Research, and by a New Opportunities Grant from the Canada Foundation for Innovation. D.L.K. is a Pappalardo Fellow.

13 December 2004; accepted 4 January 2005
Published online 13 January 2005;
10.1126/science.1108632
Include this information when citing this paper.

Optical Imaging of Neuronal Populations During Decision-Making

K. L. Briggman,[1] H. D. I. Abarbanel,[2,3] W. B. Kristan Jr.[1]*

We investigated decision-making in the leech nervous system by stimulating identical sensory inputs that sometimes elicit crawling and other times swimming. Neuronal populations were monitored with voltage-sensitive dyes after each stimulus. By quantifying the discrimination time of each neuron, we found single neurons that discriminate before the two behaviors are evident. We used principal component analysis and linear discriminant analysis to find populations of neurons that discriminated earlier than any single neuron. The analysis highlighted the neuron cell 208. Hyperpolarizing cell 208 during a stimulus biases the leech to swim; depolarizing it biases the leech to crawl or to delay swimming.

Understanding the mechanisms of behavioral choice would be a major step in bringing together neuroscience, psychology, and ethology (*1*). Research into decision-making has used several different strategies. One very productive approach is to have a primate make a sensory discrimination between very similar stimuli while the activity of neurons in various parts of the nervous system is recorded (*2*–*8*). A second approach uses choice competition: presenting an animal with two stimuli that produce mutually exclusive behaviors (choices), to see which behavior predominates (*9*). This has led to the notion that behavioral choices are hierarchical. The neuronal mechanism originally proposed to underlie behavioral hierarchies was inhibitory interactions among the neurons responsible for triggering the different behaviors (*10*). Later work has found that neurons capable of eliciting one behavior are often activated during other, sometimes conflicting, behaviors (*11*, *12*). Among other things, this observation suggests that individual decision-making neurons can be multiplexed—they contribute to choosing more than one behavior—and that they trigger behaviors by being active with other combinations of neurons.

We used a third approach to study decision-making: choice variability. We presented a nervous system with identical stimuli that repeatedly produce two different, mutually exclusive behaviors with roughly equal probabilities. This approach allowed us to focus on neurons involved in decision-making that are downstream from neurons used to make sensory discriminations.

We used the isolated central nervous system (CNS) of the medicinal leech. Motor neuron activity patterns characteristic of swimming (*13*) and crawling (*14*) can be elicited from isolated preparations by electrically stimulating peripheral nerves. Such sensory stimulation activates mechanosensory neurons in patterns that mimic touching the leech's skin (*15*). Stimulating the same kinds of mechanosensory neurons in different locations on the leech produces characteristic behaviors like swimming or crawling (*16*, *17*). We follow the terminology proposed by Schall (*18*), referring to the different behavioral outputs as choices and the process leading up to a choice as decision-making.

Previously, recording from neurons intracellularly one at a time, then stimulating them to determine their effect on the initiation of behavior, has successfully uncovered interneurons that activate swimming (*19*, *20*), crawling (*21*), and whole-body shortening (*22*). However, to explore how decisions are made by populations of neurons (*11*), we needed to record from many neurons at once (*23*). We therefore used voltage-sensitive dyes (*24*, *25*) that allowed us to record simultaneously from many neurons in a midbody segmental ganglion at a resolution better than 5 mV (*26*).

The leech CNS makes behavioral choices. The isolated leech CNS consists of a nerve cord connecting 21 segmental ganglia plus a head and tail brain (Fig. 1A). This preparation generates motor patterns that are recognizable as behaviors observed in in-

[1]Division of Biological Sciences, [2]Department of Physics, University of California–San Diego, La Jolla, CA 92093–0357, USA. [3]Marine Physical Laboratory, Scripps Institution of Oceanography, La Jolla, CA 92093–0402, USA.

*To whom correspondence should be addressed. E-mail: wkristan@ucsd.edu